Journal of Alloys and Compounds 317–318 (2001) 153–159
www.elsevier.com/locate/jallcom

Effects of Li^+ inclusion on the magnetic properties of mixed Cr/Fe oxide pillared α-zirconium phosphate materials

Mercedes Gabás[a,*], José-Ramón Ramos-Barrado[a], Antonio Jiménez-López[b], Enrique Rodríguez-Castellón[b], Josefa Mérida-Robles[b]

[a]Departamento de Física Aplicada I, Facultad de Ciencias, Universidad de Málaga, 29071 Málaga, Spain
[b]Departamento de Química Inorgánica, Facultad de Ciencias, Universidad de Málaga, 29071 Málaga, Spain

Abstract

The magnetic properties of mixed Cr/Fe 80:20 oxide pillared α-zirconium phosphate with different Li^+ exchanged contents were studied by a.c. susceptibility measurements as a function of both frequency and temperature. Also studied are magnetisation measurements as a function of both temperature and applied field. We found relaxational behaviour, which can be ascribed to the presence of very fine aggregates of mixed Fe/Cr oxide. In our study, the effect that Li^+ inclusion exerts in the material is clearly observed, probably modifying the particle size and morphology. Magnetic interactions play an important role in these compounds and their presence is deduced from experimental data.

Keywords: Pillared materials; Mixed oxide; Magnetic clusters; Magnetic relaxation

1. Introduction

Pillaring of layered compounds by insertion into the interlayer region of inorganic polycation species, and ulterior calcination, has resulted in new kinds of meso and microporous solids with large specific surface areas, thermal stability, residual cationic exchange capacity and superficial acidity for use as catalysts [1], catalyst supports [2], adsorbents [3], ion exchangers [4], etc. On the other hand, metal(IV) phosphates are appropriate matrices for this purpose owing to their high cationic exchange capacity, thermal stability and high resistance to strong acidic media. However, the number of inorganic cations capable of forming oligomers to be employed for the preparation of pillared compounds is limited. Fortunately, the use of mixed oligomers opens up many possibilities; thus, we have reported the preparation of mixed aluminium–chromium, gallium–chromium and aluminium–gallium oxides pillared into α-zirconium and α-tin phosphates [5–7]. Fe^{3+} and Cr^{3+} cations, being almost isosteric, form isomorphous oxides, which are also miscible in all composition ranges. In a previous article, we reported the synthesis and characterisation of mixed iron–chromium oxides pillared α-zirconium phosphate [8]. The high specific surface areas found for pillared materials with Fe/Cr ratios of less than 80:20 (>200 $m^2\ g^{-1}$) indicate that we have a microporous solid with some mesopore contribution. Typical pore radii found for pillared materials with low Fe/Cr ratios are between 7.5 and 15 Å.

Oxide pillared α-M(IV) phosphates (M=Sn, Zr) show a very poor ionic conductivity, but the exchanged Li^+ materials present the characteristic behaviour of an ionic conductor [9]. They show a low ionic conductivity, but the dielectric behaviour is characterised by conduction loss at low frequencies due to the movement of Li^+ ions through the pores. The special structure of these materials presents two different exchange sites for Li^+ ions: one localised in mesopores and the other in micropores, thus constituting a two potential-well system with two hopping transition processes, each with its activation energy and relaxation frequency. The Li^+ ion can only achieve long displacements through large pores because the paths across small pores are broken. These long displacements are responsible for the conducting properties, and the hopping transition into small pores — the Li^+ ion behaves as a jumping dipole — determines its dielectric properties. Both the conducting and dielectric properties show a strong dependence on Li^+ content because increasing Li^+ concentration

---

*Corresponding author. Tel.: +34-95-213-7057; fax: +34-95-213-2000.
E-mail address: mgabas@uma.es (M. Gabás).

0925-8388/01/$ – see front matter
PII: S0925-8388(00)01338-4

implies an increasing number of charge carriers, and also an increase in the interaction among ions [10]. This behaviour agrees with results reported previously for surface area and porosity and points towards a particulate or granular structure of mixed Fe/Cr oxides in these materials, where mixed oxides are located among α-ZrP layers.

For some years, the magnetic properties of ultrafine particles embedded in different matrices have been of interest to theorists and experimentalists and great effort has been made to study the fundamental and technological aspects of such systems [11]. Particle systems where the intra-particle interaction is antiferromagnetic have not been studied so extensively as those where the interaction is ferromagnetic, mainly due to the lack of technological interest in antiferromagnetic materials. Superparamagnetism and relaxation phenomena due to the blocking of antiferromagnetic particles have been observed in oxides such as NiO [12], Fe_2O_3, Cr_2O_3 [13] and MnO [14] and Co-oxides and oxyhydroxides [15]. Kodama and co-workers published a number of articles where the behaviour of antiferro- and ferrimagnetic particles were studied (see Ref. [16] and references therein). Superparamagnetic behaviour was found by Hartridge and co-workers in α-$Fe_{2-x}Cr_xO_3$ nanocrystals dispersed in a silica matrix [17,18]. We recently presented a study [19] where preliminary results suggested relaxation behaviour at low temperatures in the layered compound mixed Fe–Cr oxide pillared α-zirconium phosphate, which can be ascribed to the granular morphology of the mixed oxide. The aim of this article is the characterisation of the magnetic behaviour of the Li^+ exchanged mixed Fe/Cr oxide with a theoretical atomic ratio of 20:80, intercalated between phosphate zirconium layers, through bulk magnetic measurements.

2. Materials and experimental methods

The initial material, α-zirconium phosphate (α-ZrP), was synthesised by the sol-gel method [20]. The pillared sample was prepared by dissolving $Fe(NO_3)\cdot 9H_2O$ and $Cr(NO_3)\cdot 9H_2O$ in the atomic ratio 20:80 and the total content of cations in this solution was 10 times the cationic exchange capacity of α-ZrP. This solution was contacted with a colloidal suspension containing 1 g of α-ZrP, which was neutralised at 60% with n-propylamine and refluxed for 48 h. The Fe/Cr atomic ratio incorporated into the sample was 0.31 and the empirical formula of this sample was $Zr[Cr_{3.53}Fe_{1.10}(CH_3COO)_{1.47}OH_{10.42}](PO_4)_2\cdot 5.4H_2O$. XRD data allowed us to determine a basal spacing of 25.1 Å. Because the layer thickness of α-ZrP is 6.2 Å, the net distance between layers is 18.9 Å. However, after calcination at 673 K, it became amorphous. This material has been characterised elsewhere [8] and the results of XRD and XPS indicate that Fe^{3+} and Cr^{3+} are located between layers of α-ZrP.

High-resolution transmission electron microscopy (HRTEM) measurements were carried out using a JEOL 100 CX II transmission electron microscope. Aqueous suspensions of the samples were embedded on a holey carbon film and then cut perpendicularly to the layer sheet in order to obtain a parallel vision of the [001] lamellar plane. The HTREM micrograph (Fig. 1) shows the presence of lamellar packets composed of ribbon-like zones containing ~15–30 layers. The mutual orientation of the zones varies from almost perpendicular to small angle. This effect results in a large number of discontinuity areas and partial exfoliation of the packets. The zones are flexible and consequently their orientation may change continuously to form tangential connections. As a result, a tangle pattern composed of phosphate ribbons and voids is formed giving rise to mesoporosity.

Li^+-exchanged samples were prepared by contacting 1 g of pillared solid with a solution of LiCl for 15 h, then separating by centrifugation, washing with deionized water and drying at 333 K for 1 day. Three samples with Li^+ loadings of 50, 75 and 100% of the cationic exchange capacity were prepared. Finally, the solids were calcined at 673 K. In all cases, exchange with Li^+ causes a slight decrease in the surface area with respect to the pristine solid (209 $m^2\ g^{-1}$), the maximum difference being 13% for the fully exchanged sample. It should be noted that the quantity of mixed oxide is the same for all samples and exceeds 50 wt%.

The dielectric behaviour of the Li^+-exchanged samples, together with the very large surface areas and porosity found for all the samples, point to the fact that mixed Fe–Cr oxides are deposited between α-ZrP layers forming very small aggregates, with little distance between them (average porous radius 11.5 Å [8]).

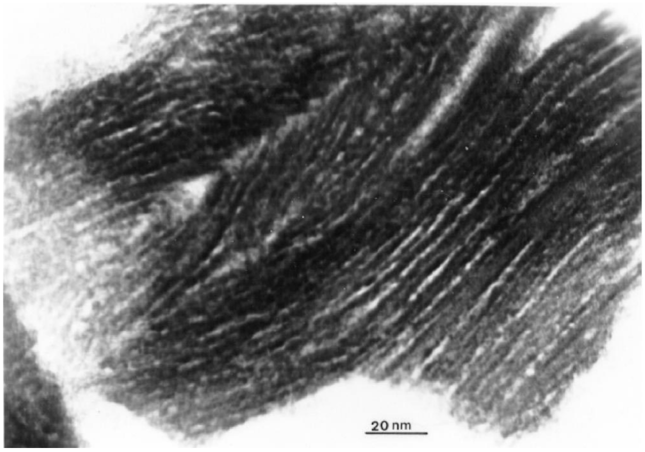

Fig. 1. HRTEM micrograph of mixed Cr/Fe 80:20 oxide pillared α-zirconium phosphate material.

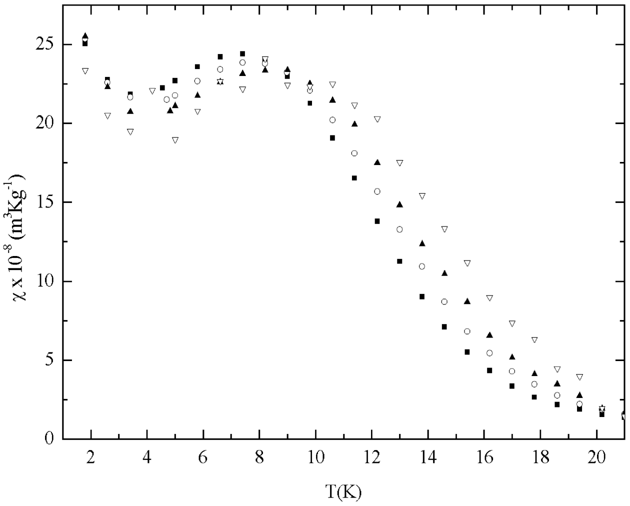

Fig. 2. Temperature dependence of the out-of-phase component of the ac susceptibility for the fully Li^+-exchanged compound at different frequencies: (■) 0.1 Hz, (○) 1 Hz, (▲) 10 Hz and (▽) 100 Hz.

Ac susceptibility and magnetisation were measured in a Quantum Design SQUID magnetometer equipped with an ac option. Measurement temperatures varied from 1.8 to 300 K. The frequency range was from 0.1 to 1000 Hz with an alternating exciting field of 4.5 Oe. Field-cooled and zero-field-cooled magnetisation were recorded in three different magnetic fields of 10, 50 and 100 Oe for all samples and magnetisation curves were measured in an applied magnetic field ranging from −50 to 50 kOe at different temperatures.

3. Results

Ac susceptibility measurements show an anomaly with slight frequency dependent behaviour of the out-of-phase component of susceptibility for all samples [19]. The frequency dependence is more evident for the fully Li^+-exchanged sample, where the relative maximum of the out-of-phase component moves to higher temperatures as frequency increases, while its magnitude diminishes (Fig. 2). This anomaly is accompanied by slight frequency dependent behaviour of the in-phase component of the susceptibility, but no maximum is detected. Low temperature behaviour shows relaxation, as expected for superparamagnetic particles when the temperature decreases and magnetic blocking occurs. However, our data show that not all the magnetic clusters become blocked when the temperature decreases to below ~10 K and this may indicate that at least a fraction of the clusters remains unblocked due to its small size.

The high temperature behaviour of the in-phase component of the susceptibility does not show any frequency dependence for any sample. For all the samples, the inverse of the in-phase ac susceptibility (Fig. 3) follows a Curie–Weiss law for temperatures higher than 200 K. Extrapolation of high temperature behaviour indicates that interactions among magnetic ions have to be antiferro-

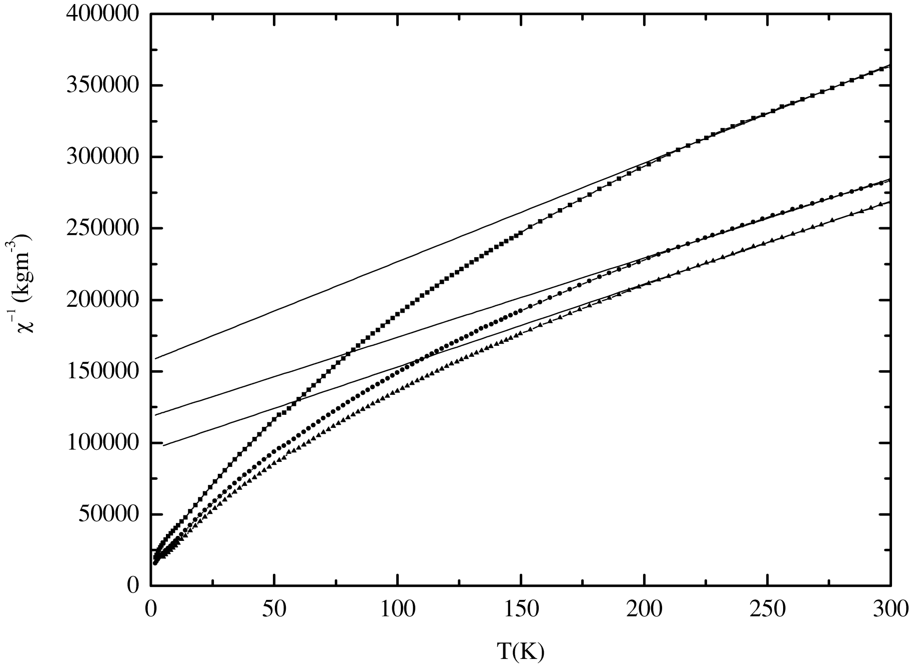

Fig. 3. Temperature dependence of the inverse of the in-phase component of the ac susceptibility for Li^+ 50% (●), Li^+ 75% (▲) and Li^+ 100% (■) at a frequency of 1 Hz. (———) Fits to the Curie–Weiss law in the high temperature region.

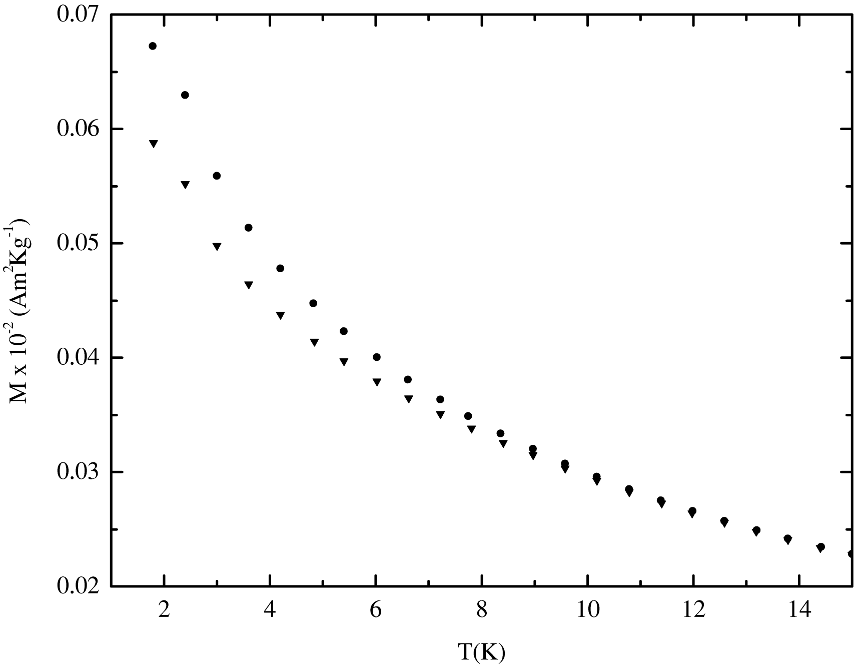

Fig. 4. Temperature dependence of magnetisation for the Li^+ 50% exchanged compound when the sample is (▼) zero-field cooled and (●) field cooled.

magnetic and that its intensity is slightly larger for the fully exchanged sample. The out-of-phase component of susceptibility is negligible for temperatures higher than the temperature at which relaxation phenomena occur.

Below a given temperature, the field-cooled (FC) and zero-field-cooled (ZFC) magnetisation curves do not superimpose (Fig. 4). The temperature for the onset of this irreversibility behaviour is similar to the temperature at which anomalies in ac susceptibility appear. The magnetisation magnitude decreases as the Li^+ content increases. For decreasing temperature, the FC magnetisation still increases in all cases, for any applied field. The same kind of behaviour is observed for the ZFC curves, where no maximum in ZFC magnetisation is detected. The form of the ZFC magnetisation curve, although always showing a tendency to increase with decreasing temperature, depends little on the Li^+ content of the sample.

Magnetisation versus applied field curves show very narrow hysteresis loops for all samples at $T = 5$ K. The coercive field is enhanced slightly with decreasing temperature and with Li^+ content. At $T = 25$ K, no hysteresis is observed for any sample. No saturation is reached for any compound, even at the highest applied field. Magnetisation curves show a very similar shape for all samples (Fig. 5).

4. Discussion

Ac susceptibility measurements versus temperature for different frequencies of the applied ac magnetic field exhibit a partial blocking phenomenon which can be associated with a superparamagnetic-like blocking of very fine magnetic particles of the Cr_2O_3/Fe_2O_3 mixed oxide present in our samples. Following Dormann et al. [11], superparamagnetic behaviour can only be present in particles with a diameter greater than 20 Å. The only information we can obtain from TEM experiments concerns the layered structure in our samples, which show a typical interlayer spacing of <18.9 Å, as deduced from XRD experiments. Although the particle size was not estimated, this distance should be considered as a limiting factor for the average diameter of our aggregates, and it would be just below the limit of the required size for observing superparamagnetic relaxation. The out-of-phase component of the ac susceptibility has a tendency to increase at the lowest temperature we can reach with our SQUID. As mentioned in the previous section, there must be a fraction of magnetic clusters that does not undergo magnetic blocking due to its very small size. The temperature at which magnetic blocking begins to occur increases with the Li^+ content of the sample. This could be an indication that particle size is affected because of the presence of this cation. A slight growth in particle size will take place, accompanied by variations in the particle shape, which will increase the shape anisotropy of the aggregates. Another possible explanation for this increase in the magnetic blocking temperature could be the interparticle magnetic interactions which will be affected by the presence of Li^+ cations. In fact, both particle size and interparticle interactions are directly related [21] and, at present, we cannot elucidate if Li^+ inclusion affects both in a direct way.

Fig. 6 depicts how the effective magnetic moment

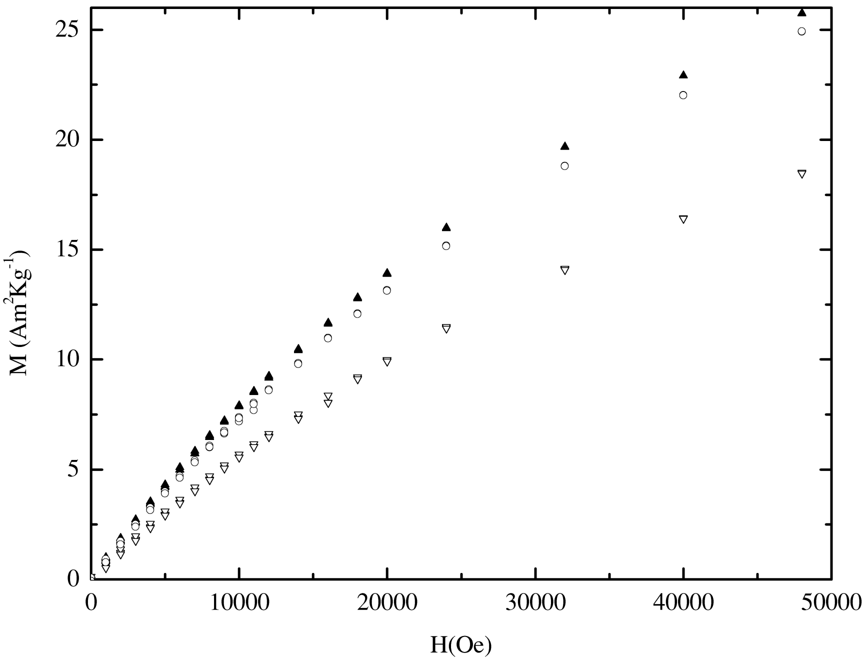

Fig. 5. Field dependence of magnetisation at $T = 5$ K for compounds: (○) Li$^+$ 50%, (▲) Li$^+$ 75% and (▽) Li$^+$ 100%.

evolves with temperature. From high temperature to ~15 K, the effective moment progressively diminishes. Due to the small size of our aggregates, long range magnetic ordering should be discarded in these materials [18], but the high magnetic oxide density favours the propagation of magnetic interactions through the interlayer space. Below 15 K, magnetic relaxation occurs and produces an inflexion in the curve. Similar behaviour was observed for all the samples.

Finite values of θ, which can be extrapolated from Fig. 3, also demonstrates the existence of static magnetic interactions. In principle, the nature of the interactions among magnetic particles and clusters can be dipolar, of exchange-type, and RKKY interactions. Although we

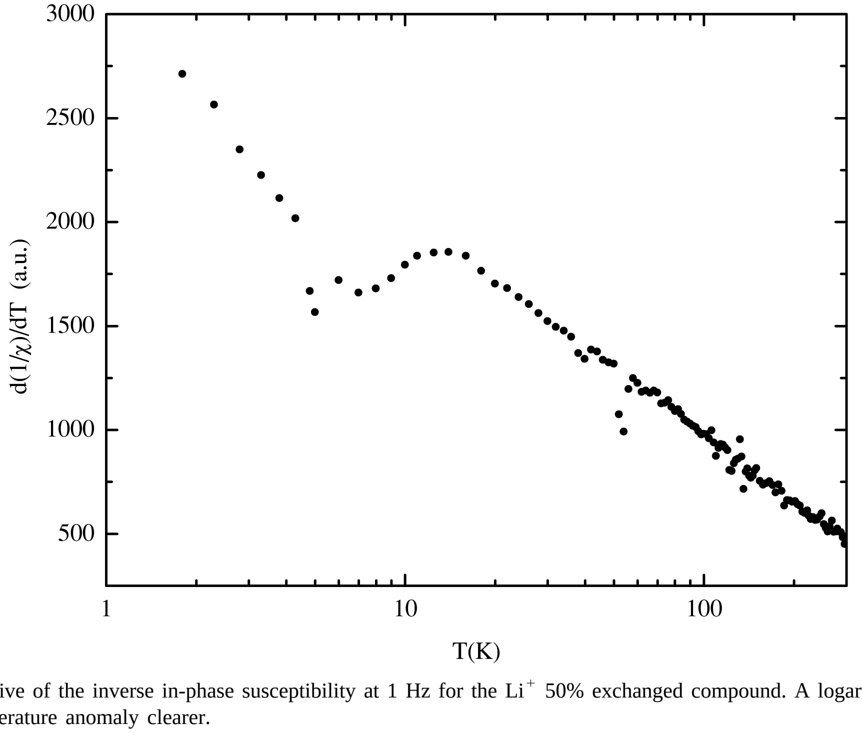

Fig. 6. Temperature derivative of the inverse in-phase susceptibility at 1 Hz for the Li$^+$ 50% exchanged compound. A logarithmic temperature scale is used to make the low temperature anomaly clearer.

cannot discard any of these, due to the high density packing of the magnetic clusters and the existence of O^{2-} anions among the magnetic ions, we propose the superexchange interaction as being dominant among the magnetic moments in these materials.

Magnetisation versus temperature measurements do not show great irreversibility behaviour as is observed in a system of superparamagnetic particles. For decreasing temperature, the field-cooled magnetisation still increases in all cases. Zero-field-cooled magnetisation also shows this increasing tendency with decreasing temperature, which can be ascribed to the coexistence of blocked and unblocked entities. The latter do not show any irreversibility phenomena and both kinds of contribution are summed throughout the whole temperature range.

In small magnetic particles, coercivity diminishes because of the increasing effect of thermal agitation on particle magnetisation. Since the energy barrier depends directly on the particle volume, an increase of the coercive field is naturally to be expected if particle size increases. In this sense, the observed increase of coercitivity with Li^+ content in our samples supports the hypothesis that the inclusion of Li^+ cations produces a growth in particle size. This is in agreement with the arguments proposed for a blocking temperature increase with Li^+ content. Although interparticle interactions affect coercitivity values, the effect does not appear in our samples, as has been observed, for example, in MnO particles [14], probably due to the small size of our aggregates. A decrease of the effective magnetic moment with temperature due to magnetic interactions is also evident in the M vs. H/T curves (Fig. 7).

In magnetisation versus applied field curves, it can be seen that none of the samples reaches saturation even at the highest applied field. The reason for the continuous increase of magnetisation with applied field could be the large surface/volume ratio of our particles, together with antiferromagnetic interactions, which will produce a complicated surface spin structure. Anomalies due to surface spin contributions have been described in anti- and ferrimagnetic particles such as NiO [22,23] and $NiFe_2O_4$ [24,25], where a spin-glass surface layer has been proposed as being responsible for the aforementioned anomalies.

5. Conclusions

The magnetic behaviour of Cr_2O_3/Fe_2O_3 mixed oxide in a α-zirconium phosphate layered structure shows a relaxation phenomenon which can be ascribed to the existence of very fine magnetic clusters of mixed oxide. Its size is limited by the interlayer space. Different Li^+ contents modify the magnetic behaviour slightly, thus it has to have an effect on particle size and/or morphology. Although some similarities to the superparamagnetic state are found, we cannot ascribe the behaviour of our materials to superparamagnetism. A complex magnetic structure originating from the large surface/volume ratio in the magnetic clusters and magnetic interactions is achieved as

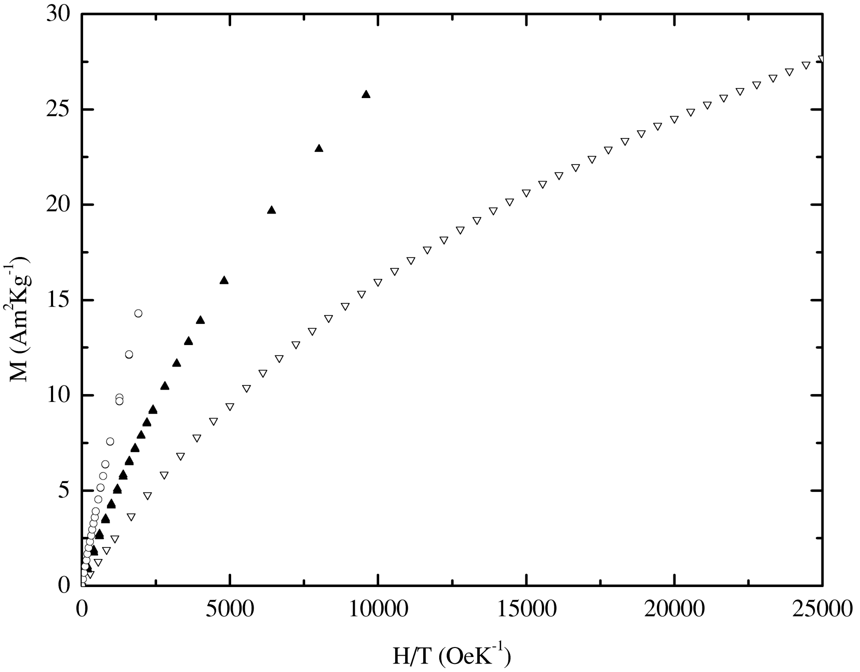

Fig. 7. Magnetisation versus H/T curves for the Li^+ 75% exchanged compound at $T = 1.8$ K (▽), 5 K (▲) and 25 K (○).

the temperature decreases and all the results point to a glass collective state of magnetic moments.

Acknowledgements

This work was supported by Junta de Andalucía (Spain) through research groups FQM192 and CICYIT, project No. Mat97-0906. Technical support with the magnetic measurements from the Servicio de Instrumentación Científica y Electrónica, Area de Medidas Magnéticas y Calibración of the University of Zaragoza is gratefully acknowledged. We are indebted to F.J. Lázaro for many fruitful discussions.

References

[1] J.M. Mérida-Robles, P. Olivera-Pastor, A. Jiménez-López, E. Rodríguez-Castellón, J. Phys. Chem. 1 (1991) 739.
[2] J.M. Mérida-Robles, P. Olivera-Pastor, A. Jiménez-López, E. Rodríguez-Castellón, J. Catal. 169 (1996) 317.
[3] R.T. Yang, M.S.A. Baksh, AIChE J. 37 (1991) 5.
[4] A. Dyer, T. Gallardo, in: P.A. Williams, M.J. Hudson (Eds.), Recent Developments in Ion Exchange, Elsevier, London, 1990, p. 75.
[5] P. Olivera-Pastor, J. Maza-Rodríguez, P. Maireles-Torres, E. Rodríguez-Castellón, A. Jiménez-López, J. Mater. Chem. 4 (1994) 179.
[6] M. Alcántara-Rodríguez, P. Olivera-Pastor, E. Rodríguez-Castellón, A. Jiménez-López, J. Mater. Chem. 6 (1996) 247.
[7] P. Braos-García, E. Rodríguez-Castellón, P. Olivera-Pastor, P. Maireles-Torres, A. Jiménez-López, J. Phys. Chem. B 102 (1998) 1673.
[8] F.J. Pérez-Reina, P. Olivera-Pastor, E. Rodríguez-Castellón, A. Jiménez-López, J. Solid State Chem. 122 (1996) 231.
[9] J.R. Ramos-Barrado, F. Martín, E. Rodríguez-Castellón, A. Jiménez-López, P. Olivera-Pastor, F. Pérez-Reina, Solid State Ionics 97 (1998) 18.
[10] J.R. Ramos-Barrado, F. Martín, F.J. Pérez-Reina, P. Maireles-Torres, P. Olivera-Pastor, E. Rodríguez-Castellón, A. Jiménez-López, J. Alloys Comp. 262/263 (1997) 281.
[11] See, for example, the review of J.L. Dormann, D. Fiorani, E. Tronc, Adv. Chem. Phys. 98 (1997) 283.
[12] J.T. Richardson, W.O. Milligan, Phys. Rev. 102 (1956) 1289.
[13] J. Cohen, K.M. Creer, R. Pauthenet, K. Srivastava, J. Phys. Soc. Jpn. 17 (Suppl. B-1) (1962) 685.
[14] S. Sako, Y. Umemura, K. Ohshima, M. Sakai, S. Bandow, J. Phys. Soc. Jpn. 65 (1996) 280.
[15] F.J. Lázaro, A. López, A. Larrea, Q.A. Pankhurst, J.M. López-Nieto, A. Corma, IEEE Trans. Magn. 34 (1998) 1030.
[16] R.H. Kodama, J. Magn. Magn. Mater. 200 (1999) 359.
[17] A.K. Bhattacharya, A. Hartridge, K.K. Mallich, C.K. Majumdar, D. Das, S.N. Chintalapudi, J. Mater. Sci. 32 (1997) 557.
[18] A. Hartridge, A.K. Bhattacharya, C.K. Majumdar, D. Das, S.N. Chintalapudi, J. Magn. Magn. Mater. 183 (1998) L1.
[19] M. Gabás, J.R. Ramos-Barrado, F.J. Pérez-Reina, E. Rodríguez-Castellón, A. Jiménez-López, J. Magn. Magn. Mater. 196/197 (1999) 218.
[20] H. Benhamza, A. Bouhaous, J. Livage, J. Chem. Phys. 88 (1991) 1875.
[21] S. Menear, A. Bradbury, R.W. Chantrell, J. Magn. Magn. Mater. 39 (1983) 17.
[22] S.A. Makhlouf, F.T. Parker, F.E. Spada, A.E. Berkowitz, J. Appl. Phys. 81 (1997) 5561.
[23] R.H. Kodama, S.A. Makhlouf, A.E. Berkowitz, Phys. Rev. Lett. 79 (1997) 1393.
[24] R.H. Kodama, A.E. Berkowitz, E.J. McNiff Jr., S. Foner, Phys. Rev. Lett. 77 (1996) 394.
[25] R.H. Kodama, A.E. Berkowitz, E.J. McNiff Jr., S. Foner, J. Appl. Phys. 81 (1997) 5552.